

# A Time-based Low Voltage Body Temperature Monitoring Unit

Karthik Ramkumar Jeyashankar, Makrand Mahalley  
Broadcom Communication Tech Pvt Ltd, Bangalore  
Email: {karthik.ramkumar.j, makrandmahalley}@gmail.com

Bharadwaj Amrutur  
Indian Institute of Science, Bangalore  
Email: amrutur@ece.iisc.ernet.in

**Abstract**—A neonatal temperature monitoring system operating in subthreshold regime that utilizes time mode signal processing is presented. Resistance deviations in a thermistor due to temperature variations are converted to delay variations that are subsequently quantized by a Delay measurement unit (DMU). The DMU does away with the need for any analog circuitry and is synthesizable entirely from digital logic. An FPGA implementation of the system demonstrates the viability of employing time mode signal processing, and measured results show that temperature resolution better than 0.1 °C can be achieved using this approach.

**Index Terms**—subthreshold design, time to digital converter, temperature measurement, sub-sampling, FPGA

## I. INTRODUCTION

Neonatal temperature monitoring systems are needed to detect conditions such as hypothermia in infants [1]. One way to implement these is to employ precision thermistors, and associated circuitry to monitor body temperature of infants. It is desirable for such systems to strive to eventually run using energy scavenged from the environment, and thus ultra low energy consumption is a key metric in these designs. Low energy consumption is also necessary in these systems to reduce errors due to self heating. The low bandwidth of temperature variations that need to be tracked in neonatal temperature monitoring makes subthreshold operation very attractive for this application.

Subthreshold circuits have attracted considerable attention in the research community in the last decade. This is primarily because they enable low energy operation for applications where high performance is not a necessity. Scaling the supply voltage causes a reduction in dynamic energy, but comes at the cost of lower speed. The circuit thus leaks for a longer time causing an increase in leakage energy per operation. In fact, research in the past has pointed to the existence of a minimum energy point where the dynamic and leakage energies balance each other to combine and result in minimum energy operation [2].

Initially, most of the temperature sensors being reported were bandgap based and were very analog intensive. Subsequently, time-based smart temperature sensors [3] have been proposed, but they have not leveraged subthreshold operation to trade off performance for low energy operation.

Operation in subthreshold brings with it the problems of low dynamic range, and increased susceptibility to process variations and mismatch [4]. In time domain signal processing,

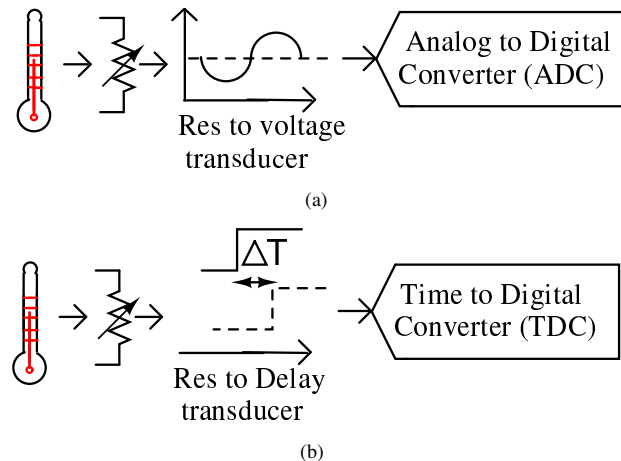


Fig. 1. Thermistor Resistance to Digital codeword conversion through (a) voltage domain, and (b) time domain

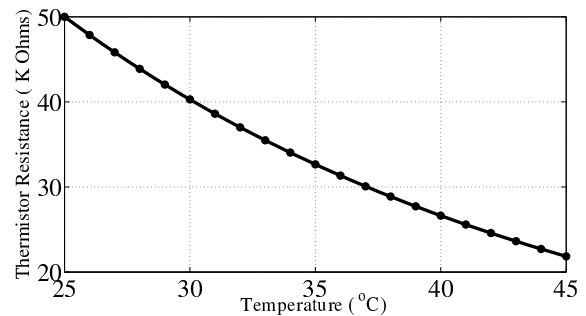


Fig. 2. Temperature vs Resistance characteristics of the thermistor over the temperature range of interest

the signal information is encoded as a delay offset with respect to a reference edge, or as a frequency offset with respect to a reference oscillator frequency, or as a modulated pulswidth. An advantage of representing signals in time domain is that the dynamic range of signals that can be represented is arbitrarily large. This is in contrast to voltage domain representation where signals are restricted to taking range of values between the supply rails, and thus their dynamic range is limited which, combined with a limit on the lowest measurable voltage step, imposes a limit on the number of bits achievable in the conversion process.

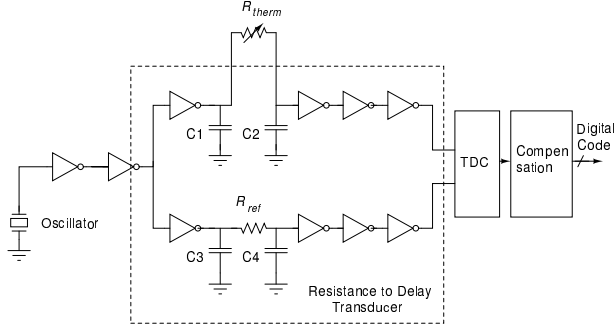


Fig. 3. Block diagram of the temp sensor that includes the crystal, resistance-to-delay transducer, and the TDC

Time domain signal processing also has the additional attractive feature of involving circuitry that is mostly-digital in nature. Low supply voltage that accompanies technology scaling makes it increasingly difficult to implement analog circuits. On the other hand, technology scaling aids digital circuits by increasing the speed of operation, and the time resolution [5]. Hence it is desirable to explore architectures that leverage this property, and which primarily rely on digital circuits to accomplish the conversion. In this regard, time based approach to data conversion has attracted significant interest in the last few years. Several works [6][7][8][9] have demonstrated time based ADCs that convert the voltage input to a delay, pulsewidth, or frequency, and which then perform quantization in the time domain.

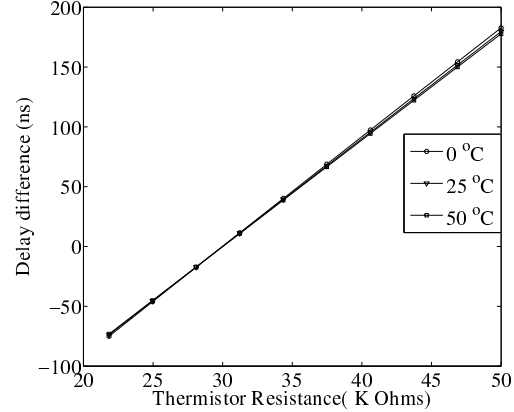
Thus subthreshold operation combined with time domain signal processing offers a very promising means of implementing body temperature monitoring systems. It combines the advantage of low energy operation that subthreshold operation makes possible, and the advantage of large dynamic range, and mostly-digital circuitry that the paradigm of time domain signal processing offers.

Figure 1(a) shows the traditional way of converting resistance (in this case, that of a thermistor) to a digital codeword by converting it to a voltage domain signal followed by an ADC. Figure 1(b) shows the time-based method, an approach that is pursued in this paper.

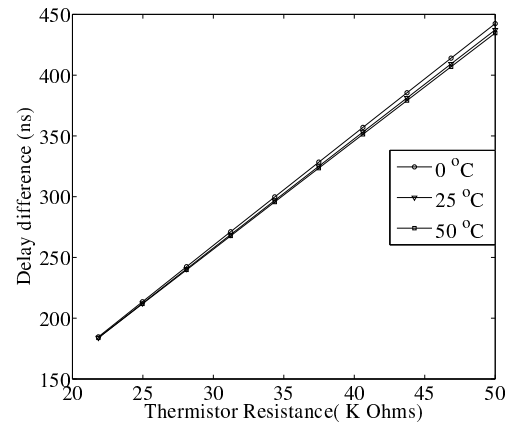
The paper is organized as follows. Section II describes the various components of the temperature monitoring system, which includes the resistance-to-delay transducer, and the delay measurement unit. In Section III, we describe our experimental setup to convert temperature information to a digital codeword, and provide measurement results in Section IV to validate this approach. Section V concludes the paper.

## II. SYSTEM OVERVIEW

The temperature monitoring unit uses a thermistor placed in direct contact with body to sense temperature. We used the US Sensor PR503J2 NTC thermistor in our system. They are ultra precise interchangeable thermistors with 0.05 °C accuracy. Figure 2 shows the temperature vs resistance characteristics



(a)



(b)

Fig. 4. Thermistor-resistance vs delay-difference at the output of the transducer across different ambient temperatures in the typical corner for (a)  $R_{ref} = 30 \text{ K}\Omega$  and (b)  $R_{ref} = 0$

of this thermistor, plotted using the data provided by the manufacturer [10].

Figure 3 shows the basic components of the temperature measurement system. The resistance of the thermistor,  $R_{therm}$ , changes in response to body temperature as shown in Fig. 2. The resistance-to-delay transducer converts this resistance information to a time domain signal, which is quantized by a time to digital converter (TDC). An oscillator generates the clock that excites the resistance-to-delay transducer. The TDC is followed by a block that compensates for the thermistor's non-linearity, and process variations. The thermistor and the reference resistor are placed off chip, and the pad capacitor plays the role of the capacitor in Fig. 3.

As shown in Fig. 3, the clock signal is buffered and fed to two paths, one of which contains the thermistor. The other path holds a reference resistor  $R_{ref}$  in place of the thermistor. Assuming the capacitors are well matched on both paths, the delays the two paths experience are proportional to the respective resistances on the paths. The delay along the

$R_{ref}$  path remains constant while that along the  $R_{therm}$  path changes with body temperature. This delay-difference/skew is then quantized through a TDC to obtain a digital representation of temperature. If the value of  $R_{therm}$  at the lower and higher end of our temperature range of interest is  $R_1$  and  $R_2$  respectively, the range of skews obtained at the output of the transducer is proportional to  $(R_1 - R_2)C$ . The purpose of using  $R_{ref}$  is described later in the paper.

Body temperature is usually maintained in the range of 36.5 °C to 37.5 °C. In infants with severe hypothermia, the body temperature can fall below 30 °C, and in patients with high fever, can exceed 41 °C. Our system was designed to support a range of 25 °C to 45 °C.

#### A. Resistance-to-Delay Transducer

Conventional approaches to converting resistance to delay make use of analog intensive circuits such as operational amplifiers, which are not suitable for ultra low voltage operation. We use a simple RC charging mechanism to convert resistance deviations to delay variations. The key considerations in the design of this transducer are choice of  $R_{therm}$  and  $R_{ref}$ , linearity of the transducer and its dynamic range, and sensitivity to process variations and variations in ambient temperature. Each of these is discussed below.

Manufacturer datasheets [10] indicate that thermistors with a larger nominal resistance at 25 °C also show larger deviations in resistance over a fixed temperature range. Hence, we chose a thermistor with a large nominal resistance (50 K $\Omega$  at 25 °C) to maximize the dynamic range of skews obtained since that relaxes the TDC requirements for the target temperature resolution. The large nominal value of the thermistor resistance  $R_{therm}$  is also necessary to ensure that the large transistor resistance at low voltages does not dominate the delays, and overwhelm the delay changes due to variations in  $R_{therm}$  with temperature.

As the temperature changes over the range of 25 °C to 45 °C, the thermistor resistance changes from 50 K $\Omega$  to about 22 K $\Omega$ . Figure 4(a) shows the delay difference produced at the output of the resistance-to-delay transducer (which in turn is measured by the TDC) in response to this resistance change when all the capacitors shown in the figure are 10pf,  $R_{ref} = 30$  K $\Omega$  and  $V_{dd} = 350$  mV. The simulation was done in UMC 0.13  $\mu$ m CMOS technology. The temperature coefficient of  $R_{ref}$  was set to 25 ppm/°C in the simulation since precision metal-film resistors with this temperature coefficient are commercially available. When the ambient temperature is 25 °C, the resistance-to-delay transducer produces a skew range of 253 ns for a body temperature variation from 25 °C to 45 °C. The transducer is linear in our temperature range of interest, with the maximum residual error from a linear fit being 0.3 ns, and this occurs at the extremes of the temperature range. Fig. 4(b) plots the transducer's transfer characteristics when the reference resistor is an electrical short.

It is important that changes in the ambient temperature do not affect the measurement of the body temperature. The ambient temperature is assumed to vary over a range of 0 °C

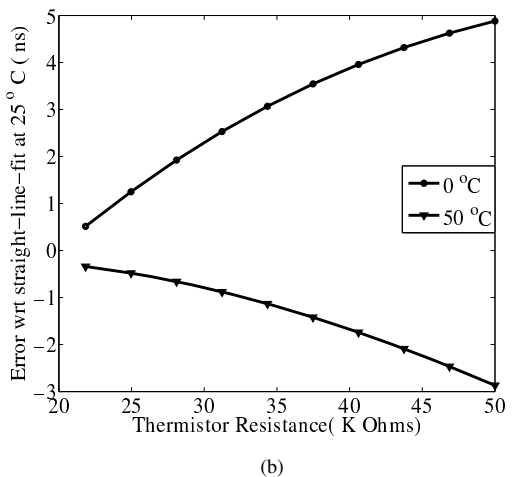
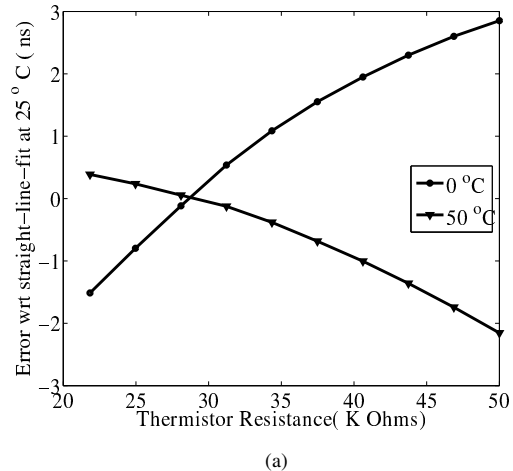


Fig. 5. Residual error from a straight line fit obtained at an ambient temperature of 25 °C for (a)  $R_{ref} = 30$  K $\Omega$ , and (b)  $R_{ref} = 0$

to 50 °C independent of the body temperature. The buffers in the resistance-to-delay transducer in Fig. 3 are subjected to this temperature change in the simulation. As the ambient temperature changes over 0 °C to 50 °C, the skew range at the output of the transducer varies from 251 ns to 258 ns.

It is desirable to have least measurement error while measuring body temperatures close to the nominal value of 37 °C. Simulations show that effects of ambient-temperature variations have the least impact while measuring body-temperature at which  $R_{therm}$  matches  $R_{ref}$ . Based on this, the reference resistor was chosen to be 30 K $\Omega$ . To quantify this, we find a linear fit for the transducer's characteristics in Fig. 4 when the ambient temperature is 25 °C. We then compute the deviation from this straight line fit for the other two curves in Fig. 4 that correspond to ambient temperatures of 0 °C and 50 °C. This deviation represents the error introduced due to changing ambient conditions as a result of calibrating the transducer only once at an ambient temperature of 25 °C. Fig 5(a) shows

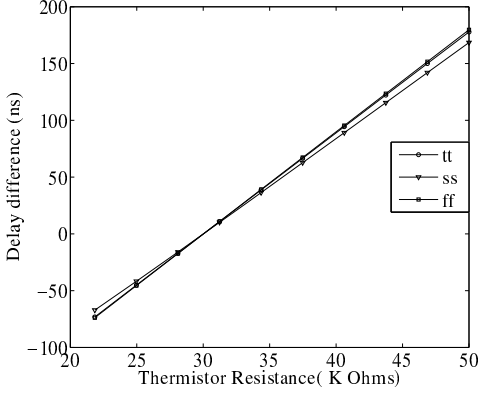


Fig. 6. Delay along the thermistor and the reference resistor paths across different process corners for an ambient temperature of 25 °C. The range of skews produced by the transducer is largely unaffected by process variations as well.

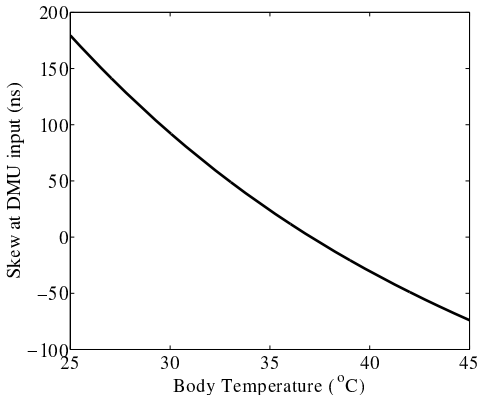


Fig. 7. The composite Body-temperature vs Delay characteristics obtained by combining the characteristics of the thermistor and the resistance-to-delay transducer. Ambient temperature changes cause very minor change in these characteristics.

the residual error when  $R_{ref} = 30 \text{ K}\Omega$  is used. Fig 5(b) plots the residual error when  $R_{ref}$  is chosen to be 0. Choosing  $R_{ref}$  to be  $30 \text{ K}\Omega$  minimizes error when  $R_{therm}$  is  $30 \text{ K}\Omega$  ( which occurs at body temperature of  $37 \text{ }^\circ\text{C}$ ).  $R_{ref}$  can be thought of as setting the 'bias-point' for the transducer, and the transducer output is least sensitive to ambient temperature changes when the thermistor resistance stays close to this bias-point.

The transducer's characteristics are largely insensitive to ambient temperature variations as seen in Fig. 4 . Temperature variations affect delays of buffers on both the thermistor as well as the reference resistor paths in Fig. 3 equally, and hence appears as a common mode component which gets canceled out as the TDC looks at only the differences in edge spacings. Fig. 6 shows that this is true of process variations as well. Thus, the resistance-to-delay transducer produces a range of skews at the input of TDC that is largely invariant to ambient temperature changes as well as process variations . Further, since an RC charging mechanism is employed, the delays are

tolerant to supply voltage changes as well making this a robust transducer that functions well at low voltages.

### B. Delay Measurement Unit

The TDC in this application is based on the Delay measurement unit [11] shown in Fig. 8. The DMU measures the skew between two periodic inputs, and represents it as a digital codeword. Owing to its all-digital nature, it is synthesizable on both the ASIC and FPGA. The synthesis tool could be directed to avoid gates with high fan-in to result in a design that can function down to very low voltages [4]. Its all-digital nature also eliminates problems of non-linearity and mismatch that analog circuits typically face at low voltages.

The DMU utilizes the principle of sub-sampling for its operation. The two input edges between which the skew needs to be measured, are sampled with a near-frequency asynchronous sampling clock. This results in beat signals at the output of the samplers that are skewed on a larger time scale [11]. The beat signals are then processed with de-bounce and masking state machines to retain skew information only in the rising edges of the inputs. The histogram of arithmetic difference of the beat signals is then computed. This decouples the relationship of clock jitter to minimum measurable skew, with the measurable skew being limited only by the measurement time, and not by jitter. This property is also valuable in subthreshold operation where slow edge rates and poor jitter are inevitable.

The resistance-to-delay transducer is excited with a periodic signal with period  $T$ , as shown in Fig. 8. The two signals at the output of the transducer are sampled by a separate sampling clock, which has a slightly different clock period  $T_s = T + \Delta T$ . The sampled outputs,  $q1$  and  $q2$  will be beat signals whose period is  $T * T_s / \Delta T$ . The input skew  $\delta$  similarly undergoes magnification to be  $\delta * T_s / \Delta T$ . The difference between the sampler outputs is averaged over  $2^k$  samples to obtain an estimate of the skew.

$$S = \frac{1}{2^k} \sum_{i=1}^k X_i \quad (1)$$

where  $X_i$  is the arithmetic difference between the  $i^{th}$  sampler outputs. It was also shown in [11] that

$$\mathbb{E}(S) = \frac{\delta}{T} \quad (2)$$

### C. Calibration

The system needs to be calibrated before use to accurately interpret the sensor output in the face of process variations. As long as the clock sources are stable with varying ambient conditions, the DMU's characteristics will remain unaffected due to its all-digital nature. The resistance-to-delay transducer is less sensitive to ambient temperature variations than to process variations. Calibrating the sensor once at an ambient temperature of  $25 \text{ }^\circ\text{C}$  leads to less than  $0.01 \text{ }^\circ\text{C}$  measurement error (while measuring body temperatures higher than  $34 \text{ }^\circ\text{C}$ ) when the ambient temperature then changes in the range of  $0 \text{ }^\circ\text{C}$  to  $50 \text{ }^\circ\text{C}$ .

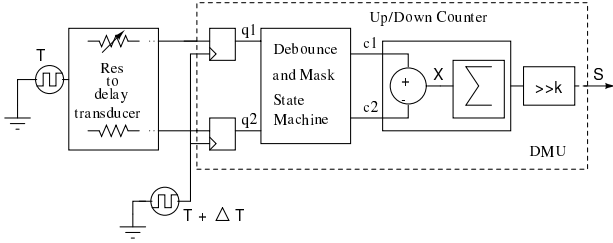


Fig. 8. The TDC is based on the Delay measurement unit (DMU). It outputs a digital codeword that represents the skew between the two inputs as a fraction of the input period.

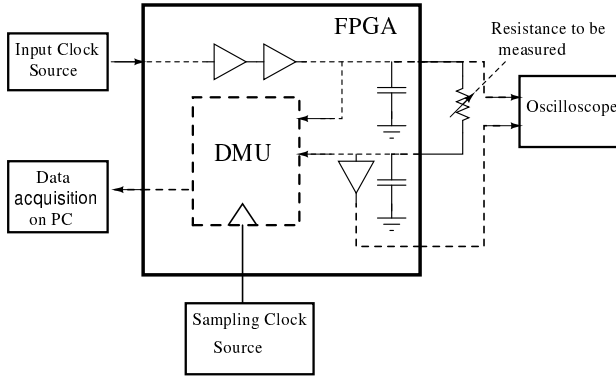


Fig. 9. Measurement setup in the lab

Process variations will primarily affect the system in two ways - They might lead to a systematic mismatch between the reference-resistor and the thermistor paths which leads to an offset at the DMU input. Also they will impact the slope of the resistance-to-delay transducer. This can be seen in Fig. 6, where we see that the slope of the transducer's characteristics is almost the same in the typical and fast corners, but is different in the slow corner. A one-time calibration can be done at two different body-temperatures to determine the slope and offset of the temperature sensor, from which a linear fit can be obtained. To reduce calibration effort, two precise off-chip resistances with low-temperature coefficient could be used to mimic the thermistor's behavior at those temperatures. During the calibration phase, two measurements are obtained by using these resistors in a sequence to perform two point calibration.

The non-linearity of the thermistor's characteristics needs to be accounted for while interpreting the DMU's output. However this is a fixed non-linearity and interchangeability tolerance is assured by the manufacturer to be  $\pm 0.05$  °C from 0 °C to 50 °C. Fig. 7 shows the simulated composite characteristics of the temperature sensor that incorporates the thermistor's temperature vs resistance characteristic, and the transducer's resistance vs delay characteristic. It is obtained from combining the information from Fig. 2 and Fig. 4. Hence the calibration procedure primarily calibrates for changes in the resistance-to-delay transducer's characteristics due to chip-to-chip variations.

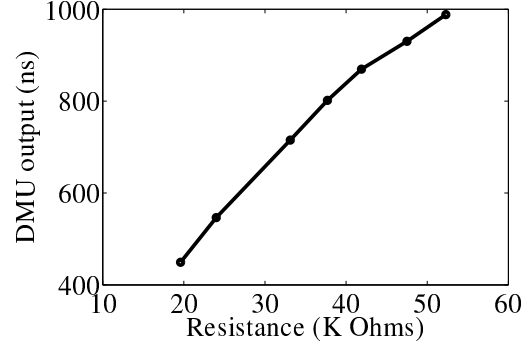


Fig. 10. Output of DMU over the resistance range of interest

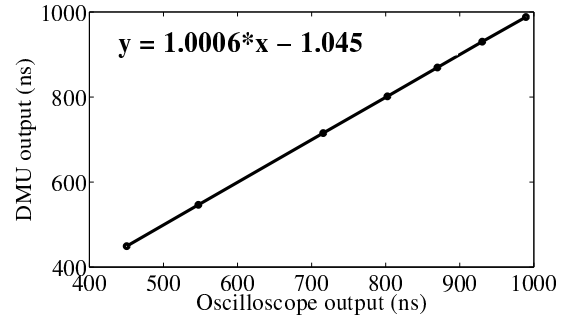


Fig. 11. Correlation of the DMU output to the oscilloscope output over the resistance range of interest.

### III. EXPERIMENTAL SETUP

Fig. 9 shows the experimental setup. We have used two asynchronous signal generators, Agilent 80 MHz 33250A and Agilent 120 MHz 81150A to provide 2 asynchronous clocks of very close frequency (100 KHz and 99.5 KHz) with  $T/\Delta T$  ratio close to 200. The input clock source was buffered through the FPGA to drive the resistor, which in conjunction with the pad capacitance produces a delay. This delay is quantized by the DMU, and the DMU's output is compared against the oscilloscope (Agilent DSO90404A) output to verify its correctness.

This measurement setup differs from the system block diagram in Fig. 3 in two aspects. Firstly, for ease of implementation, the reference resistor is omitted in the measurement setup. This will not affect the precision of results. Secondly, the FPGA operates at nominal  $V_{dd}$ , and not at subthreshold. As was described earlier, both the resistance-to-delay transducer as well as the DMU are expected to function well at low voltages. Further the range of skews produced by the resistance-to-delay transducer is almost independent of  $V_{dd}$ . Also, the DMU resolution is dependent on the time-period difference between the two clocks, and the measurement time. Thus this design lends itself well to low voltage operation. The FPGA implementation illustrates the all-digital nature of this approach and validates the feasibility of this architecture.

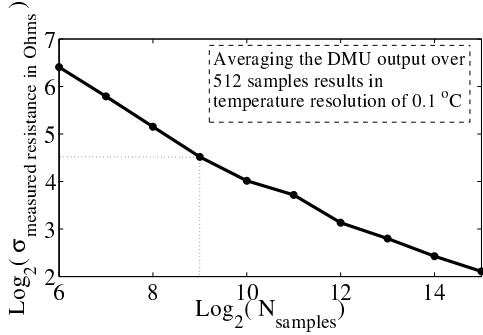


Fig. 12. Measured standard deviation as a function of number of samples

#### IV. MEASUREMENT RESULTS

As input clock source of 100 KHz was used as source, and the sampling clock frequency was chosen to be 99.5 KHz. This gives us  $T = 10 \mu\text{s}$ , and  $\Delta T = 50.25 \text{ ns}$ . The pad capacitance at the FPGA inputs was found to be large and this proves to be an advantage as it results in a large dynamic range of skews obtained for a given temperature variation. Experiments also revealed that the variation of pad capacitance across different pins was quite small, and thus the design could be easily shifted to use a different pin without affecting the results.

Over the temperature range of 25 °C to 45 °C, the thermistor resistance varies between 50 K $\Omega$  and 22 K $\Omega$ . Fig. 10 shows the DMU output (translated to equivalent measured delay) over this temperature range. On averaging the result over  $2^{15}$  samples, the DMU measures resistance with a resolution of 25  $\Omega$ , which translates to temperature resolution of 0.02 °C. Averaging over  $2^9$  samples results in a temperature resolution of 0.1 °C. The DMU output is linear in the resistance range of 24 K $\Omega$  to 42 K $\Omega$ . This corresponds to high linearity in the body temperature range of 29 °C to 42 °C.

A change in  $R_{therm}$  in response to body temperature change also causes changes in the slew rate at which the pad capacitor node transitions. These slew rate changes impact the delay of succeeding buffer, the delay of which should be ideally invariant to variations in  $R_{therm}$ . We believe this to be the cause for non-linearity at the extremes of the characteristics in Fig. 10. The measured standard deviation of the DMU output was observed to be in the range of 0.07 ns (equivalently 0.0031 °C or 4.5  $\Omega$ ) to 36 ns (equivalently 1.63 °C or 2.29 K $\Omega$ ) depending on the measurement time of 320 ms ( $2^{15}$  samples) to 0.64 ms (1 sample) respectively.

Figure 11 shows the correlation of the DMU results to oscilloscope measurements. The residual difference is observed to be less than 1.1 ns (equivalently 0.05 °C) when the output of DMU is averaged over  $2^{15}$  samples. The DMU output matches very well with that measured by the scope. The non-linearity in Fig. 10 is thus largely due to the transducer's characteristics. In [11], it was shown that the standard deviation is bounded by the number of samples  $2^k$  as

$$S \leq \frac{1}{\sqrt{2^{k+1}}} \quad (3)$$

Figure 12 shows the measured standard deviation of the resistance as the number of samples over which the output is averaged is varied. The standard deviation of the output reduces with square root of the number of samples. This provision to control the number of samples being averaged provides a useful knob to trade off resolution for measurement time, and thus energy (as leakage energy scales with measurement time). We find that averaging the DMU output over  $2^9$  samples is sufficient to obtain a temperature resolution of 0.1 °C.

#### V. CONCLUSION

Subthreshold operation in conjunction with time mode signal processing is an attractive means of implementing body temperature measurement systems. The resistance-to-delay transducer was shown to be tolerant to ambient temperature changes as well as process variations, and its output range is independent of supply voltage. The digital nature of DMU makes it well suited for synthesis as well as easy portability to newer nodes. An FPGA implementation validates this approach and the measured results indicate that resolution better than 0.1 °C can be achieved using this approach.

#### ACKNOWLEDGMENT

The authors would like to thank K R Viveka for valuable discussions, and the Robert Bosch Center for Cyber-Physical Systems at IISc, for funding support.

#### REFERENCES

- [1] E. McCall, A. F., H. H.L., J. J.G., and V. S., "Interventions to prevent hypothermia at birth in preterm and/or low birthweight infants." *Cochrane Database of Systematic Reviews*, vol. 1, no. CD004210, DOI: 10.1002/14651858.CD004210.pub3., Oct 2008.
- [2] A. Wang, A. Chandrakasan, and S. Kosonocky, "Optimal supply and threshold scaling for subthreshold cmos circuits," in *VLSI, 2002. Proceedings. IEEE Computer Society Annual Symposium on*, 2002, pp. 5–9.
- [3] P. Chen, C.-C. Chen, C.-C. Tsai, and W.-F. Lu, "A time-to-digital-converter-based cmos smart temperature sensor." *Solid-State Circuits, IEEE Journal of*, vol. 40, no. 8, pp. 1642–1648, Aug. 2005.
- [4] M. Alioti, "Ultra-low power vlsi circuit design demystified and explained: A tutorial." *Circuits and Systems I: Regular Papers, IEEE Transactions on*, vol. 59, no. 1, pp. 3–29, jan. 2012.
- [5] R. Staszewski et al., "All-digital tx frequency synthesizer and discrete-time receiver for bluetooth radio in 130-nm cmos," *Solid-State Circuits, IEEE Journal of*, vol. 39, no. 12, pp. 2278–2291, dec. 2004.
- [6] T. Watanabe, T. Mizuno, and Y. Makino, "An all-digital analog-to-digital converter with 12- $\mu\text{V}/\text{lsb}$  using moving-average filtering," *Solid-State Circuits, IEEE Journal of*, vol. 38, no. 1, pp. 120–125, jan 2003.
- [7] M. Straayer and M. Perrott, "A 12-bit, 10-mhz bandwidth, continuous-time sigma delta adc with a 5-bit, 950-ms/s vco-based quantizer," *Solid-State Circuits, IEEE Journal of*, vol. 43, no. 4, pp. 805–814, april 2008.
- [8] C. Taillefer and G. Roberts, "Delta-sigma a/d conversion via time-mode signal processing," *Circuits and Systems I: Regular Papers, IEEE Transactions on*, vol. 56, no. 9, pp. 1908–1920, sept. 2009.
- [9] G. Li, Y. Tousi, A. Hassibi, and E. Afshari, "Delay-line-based analog-to-digital converters," *Circuits and Systems II: Express Briefs, IEEE Transactions on*, vol. 56, no. 6, pp. 464–468, june 2009.
- [10] NTC Resistance-Temperature Chart. [Online]. Available: [http://ussensor.com/rt\\_charts/PR503J2.htm](http://ussensor.com/rt_charts/PR503J2.htm)
- [11] B. Amrutur, P. Das, and R. Vasudevamurthy, "0.84 ps resolution clock skew measurement via subsampling," *Very Large Scale Integration (VLSI) Systems, IEEE Transactions on*, vol. 19, no. 12, pp. 2267–2275, dec. 2011.